Homogeneous Low Spatial Frequency LIPSS on Dielectric Materials Generated by Beam-Shaped Femtosecond Pulsed Laser Irradiation

Simon Schwarz[1], Stefan Rung[1], Cemal Esen[2] and Ralf Hellmann[1]

[1] *Applied Laser and Photonics Group, University of Applied Sciences Aschaffenburg, Wuerzburger Strasse 45, 63743 Aschaffenburg, Germany*
E-mail: Simon.Schwarz@h-ab.de
[2] *Applied Laser Technologies, Ruhr-University Bochum, Universitaetsstrasse 150, Bochum 44801, Germany*

We report on the generation of homogenous low spatial frequency LIPSS on fused silica and sapphire with beam-shaped femtosecond pulsed laser irradiation. For the silica specimen, the periodicities of the LSFL generated by a Gaussian and a Top-Hat beam profile are compared with regard to the applied fluence, pulse overlap and angle of incidence. For both profiles, an increasing periodicity is found for an increasing pulse overlap and a decreasing periodicity for an increasing angle of incidence, in turn facilitating a fine-adjustment of the LSFL periodicity for potential applications. Furthermore, for a homogenous surface coverage with LSFL, the silica sample is rotated 40° for an angular irradiation, improving the quality of the periodic structures for Gaussian irradiation. Applying the beam-shaped Top-Hat laser profile, superior LSFL with increased line width are observed. For sapphire, we focus on the generation of one-dimensional structures along straight lines with respect to different scanning directions, being either parallel or orthogonal to the laser polarization. We found an excellent quality for parallel scanning using Top-Hat beam profile as well as an increased line width as compared to Gaussian beam profile. From an applicable point of view, these high-quality structures lead to the next step texturing entire surfaces of transparent materials with homogenous microstructures for a specific adaption of the cell growth or wettability.

DOI: 10.2961/jlmn.2018.02.0007
Keywords: LIPSS, LSFL, femtosecond, dielectric, fused silica, sapphire, beam-shaping, top-hat

1. Introduction

Since the first observation of laser-induced periodic surface structures (LIPSS) in 1965 by Birnbaum [1], both their formation mechanisms and their manifold applications are topic of intensive research. The formation of LIPSS is typically observed upon the irradiation of solids with polarized laser light, having a fluence near the materials ablation threshold [2-4]. In literature, two types of LIPSS are generally distinguished by their spatial periodicity Λ, namely low spatial frequency LIPSS (LSFL) having a periodicity close to the laser wavelength λ ($\Lambda_{LSFL} \approx \lambda$) and high spatial frequency LIPSS (HSFL) having a periodicity significantly smaller than the laser wavelength ($\Lambda_{HSFL} \ll \lambda$) [4-6]. The generation of LSFL is commonly described by the interference of a surface scattered wave generated by the incident laser light and the electromagnetic field of the laser [7]. This surface scattered wave was later associated to surface plasmon polaritons (SPP) [4]. While the SPP theory forms the basis of recent examinations, no established theory exists for the generation of HSFL [8, 9].

The formation of LIPSS has been demonstrated on all solid material classes, i.e. metals [3, 10, 11], semiconductors [1, 4, 12] and dielectrics [6, 13, 14]. Along this way, it has been shown that LIPSS alter the wetting behaviour [3, 10, 15], influence cell growth [16-18], modify tribological characteristics [12, 19, 20], and alter the reflection properties of thus structured surfaces [21]. With particular respect to transmission light microscopy in medical and biotechnological applications, the possibility to influence cell growth on glass object slides and specimen holders provides enormous potential for LSFL.

Against this background, we report on the generation of one-dimensional LSFL (1D-LSFL) on fused silica and sapphire. Compared to metals and semiconductors, these materials have no free charge carriers that are required for the generation of SPP. However, upon multiphoton absorption and avalanche ionization, free charge carriers can also be generated in dielectric materials [22], tuning the irradiated substrate surface region into a metallic type state [9, 23, 24].

Punctual LSFL on dielectric materials have previously been demonstrated in several publications for both fused silica [6, 25, 26] and sapphire [14, 27, 28]. From an applicative point of view, the transfer from punctual LSFL into straight lines is an essential step towards functionalizing specific regions of a specimen holder and a prerequisite to structure entire surfaces. In previous publications, the authors have already demonstrated this important transfer from punctual LSFL into one-dimensional LSFL (1D-LSFL) for fused silica and sapphire [13, 29]. To increase the quality of these structures, here we specifically focus on the generation of 1D-LSFL with beam-shaped femtosecond laser pulses. Therefore, the Gaussian beam is transformed into a Top-Hat

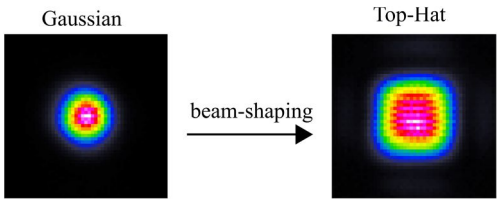

Fig. 1 Gaussian and Top-Hat beam-shaped intensity profiles.

beam profile, offering a more homogeneous intensity distribution. The quality and structural properties are compared for 1D-LSFL being generated by both beam profiles on fused silica and sapphire.

2. Experimental

In our experimental study, a Yb:KGW femtosecond pulsed laser (Pharos, Light Conversion) having a wavelength of 1030 nm is used. The laser is equipped to a micromachining system including a galvo scanner (RTA AR800 2G+, Newson) with an f-Θ-lens having a focal length of 100 mm. To alter the beam profile, a diffractive beam shaper (ST-225-I-Y-A, Holo/Or) is used. Figure 1 shows both, a focused Gaussian beam profile and the beam-shaped Top-Hat profile. The focal diameter d_0 of the Gaussian beam and the edge length l_0 of the Top-Hat profile are 31 µm ($1/e^2$) and 45 µm ($1/e^2$) as being measured by a high resolution CCD camera (UI-1490SE-M-GL, IDS). The fluence is calculated with $\Phi = E_p/(\pi * r_0^2)$ for the Gaussian and $\Phi = E_p/l_0^2$ for the Top-Hat beam, while r_0 is the focal beam radius and E_p the pulse energy. The pulse overlap PO for the scanning laser is determined by the overlapping diameters for the Gaussian and the overlapping edge lengths for the Top-Hat beam profile. An external attenuator is used to alter the pulse energy, while the pulse duration is 230 fs (FWHM, measured after laser aperture) in our study with a pulse repetition rate of 50 kHz. Two materials namely fused silica (GVB Solutions in Glass) and sapphire (UQG Optics) are chosen as prominent candidates in LIPSS generation on dielectric materials. To analyse the ablated structures in detail, a scanning electron microscope (Phenom ProX, Phenom-World) and a transmitted light microscope (DM6000 M, Leica) are used.

3. Results and discussion

3.1 Fused Silica

To get acquainted with the properties of the LSFL, first the influence of the fluence, the pulse overlap and the angle of incidence Θ is evaluated for both beam profiles. Figure 2 shows exemplarily scanning electron microscopy (SEM) images for different 1D-LSFL on fused silica and the corresponding experimental setups. An example of good one-dimensional LSFL for the Gaussian beam is shown in figure 2 (a) generated with 2.53 J/cm² at normal incidence. The LSFL and the line rim reveal damage and inhomogeneity while the orientation of the LSFL is parallel to the polarization, a behaviour typically observed for punctual LSFL on fused silica [6, 25, 26]. Examples of 1D-LSFL generate at angular incidence (Θ = 40°) for the Gaussian and the Top-Hat beam profile are exemplarily shown in figure 2 (b) and (c). For the structuring, the polarization is kept orthogonal to the scanning direction as shown in the schematics. Obviously, the angle of incidence has a significant influence on

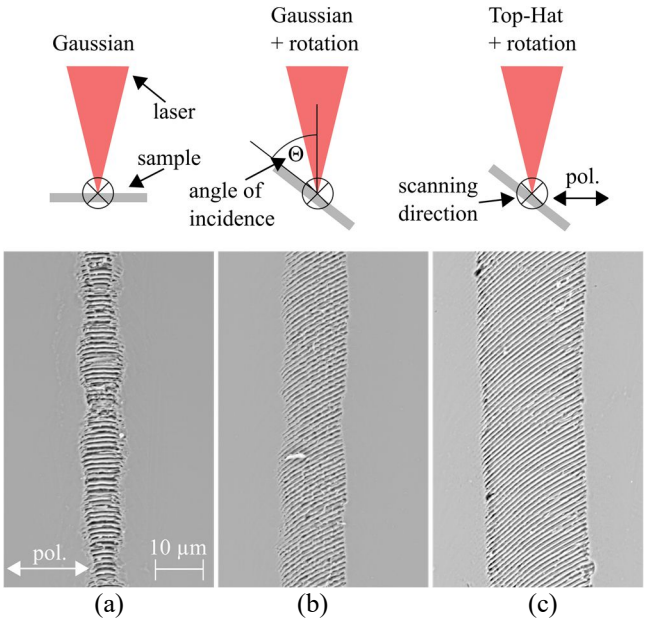

Fig. 2 SEM images of 1D-LSFL on fused silica and their experimental setups generated with different beam profiles and angle of incidence (a) Gaussian beam at Θ = 0°, (b) Gaussian beam at Θ = 40° and (c) Top-Hat at Θ = 40°.

the periodicity and orientation of the LSFL as well as their quality, i.e. more homogenous and less damaged LSFL. For the Top-Hat beam profile the quality is further improved compared to the Gaussian. Furthermore, the line width is increased due to the larger spot size.

To evaluate the influence of the fluence on the periodicities of the generated structures, the scanning speed is set to 200 mm/s leading to a pulse overlap of 87% for the Gaussian and 91% for the Top-Hat beam profile. The applied fluence is varied between 2.53 J/cm² and 3.43 J/cm² for the Gaussian and 2.55 J/cm² and 3.66 J/cm² for the Top-Hat profile, respectively. Please note, while the fluence regimen for the generation of 1D-LSFL is nearly the same for both beam profiles, the corresponding pulse energies are between 19.1 µJ and 25.9 µJ for the Gaussian and 51.6 µJ and 74.1 µJ for the Top-Hat beam profile. The significantly increased pulse energy for the Top-Hat accounts for the larger spot size (cf. section 2). Figure 3 shows the influence of the fluence on Λ_{LSFL}. As Λ_{LSFL} slightly decreases from 1101 nm to 1081 nm for the Gaussian beam, no distinct trend is apparent for the Top-Hat profile. Furthermore, for both profiles, the periodicities reveal nearly the same values with Λ_{LSFL} being larger than the wavelength of the laser (1030 nm).

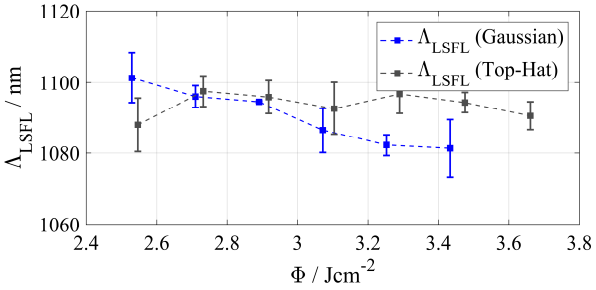

Fig. 3 Influence of the fluence on the LSFL periodicities for Gaussian (blue) and Top-Hat (grey) for orthogonal incidence (Θ = 0°).

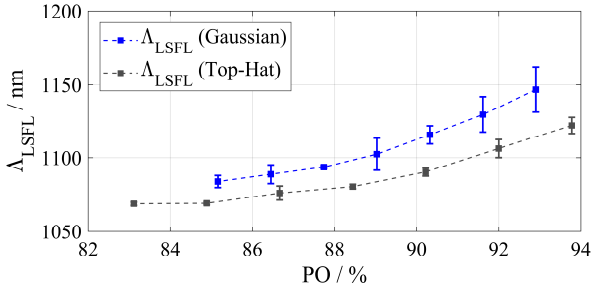

Fig. 4 Influence of the pulse overlap on the LSFL periodicities for Gaussian (blue, Φ = 2.86 J/cm², E_p = 21.6 µJ) and Top-Hat (grey, Φ = 3.66 J/cm², E_p = 74.1 µJ) at Θ = 0°.

The influence of the pulse overlap on the LSFL periodicities is presented in figure 4 generated with constant fluences of 2.86 J/cm² (Gaussian beam profile, E_p = 21.6 µJ) and 3.66 J/cm² (Top-Hat beam profile, E_p = 74.1µJ). The PO shown in figure 4 correspond to scanning speeds between 110 mm/s and 230 mm/s for the Gaussian and 140 mm/s and 380 mm/s for the Top-Hat beam profile. For both beam profiles, Λ_{LSFL} increases with increasing pulse overlap, from 1084 nm to 1147 nm for the Gaussian and from 1069 nm to 1122 nm for the Top-Hat profile. Therefore, the pulse overlap and thus the scanning speed can effectively be used to adjust the required periodicity of the structures in a range of over 60 nm for the Gaussian and 50 nm for the Top-Hat profile. Furthermore, over the entire range, Λ_{LSFL} reveals slightly increased values for the Gaussian beam profile compared to the Top-Hat at the same pulse overlap.

In a previous study [13], the authors reported on an increasing quality of 1D-LSFL for structuring fused silica with different angles of irradiation and found a decreasing periodicity of the LSFL beside a rotation of the LSFL for increasing Θ. In addition, the quality of the LSFL improves at an intermediate angle of incidence and deteriorates again at large angles. Figure 2 (b) and (c) show schematics of the experiments under angular irradiation. Again, here we compare the Top-Hat beam profile with the Gaussian one while for both the scanning speed is set to 200 mm/s. Please note, the fluence has to be adapted with increasing angle of incidence to ensure a successful structuring, e.g., 3.13 J/cm² for the Gaussian and 2.92 J/cm² for the Top-Hat beam profile at Θ = 40°. Figure 5 (a) shows the influence of Θ on the orientation of the LSFL (scanning direction remains orthogonal to polarization of the laser, see schematic in figure 2 (b) and (c)). Increasing the angle of irradiation from 0° up to 70°, leads to a rotation of the LSFL of about 40° over the entire range for both beam profiles, a behaviour being still under research. Furthermore, Λ_{LSFL} decreases with increasing angle of incidence from about 1100 nm to 800 nm for both the Gaussian and the Top-Hat profile, leading to an adjustment of the LSFL periodicity in a range of about 300 nm (figure 5 (b)).

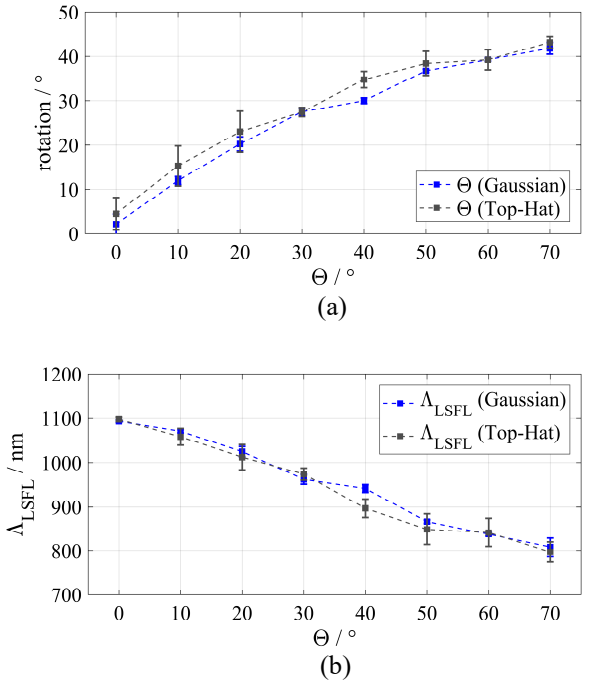

Fig. 5 Influence of the angle of incidence for Gaussian (blue) and Top-Hat (grey) beam profiles on (a) the LSFL periodicities and (b) rotation angle.

However, beside the required pulse energy for the generation of 1D-LSFL, no significant difference exists for their periodicities and orientation between the several beam profiles and the evaluated parameters i.e. fluence, pulse overlap and angle of incidence. Nevertheless, structuring fused silica with a Gaussian beam at angular irradiation leads to an increased quality of the LSFL, which is further improved by applying a Top-Hat beam profile.

3.2 Sapphire

Due to the experiments on fused silica, which showed that the investigated parameters (pulse overlap, fluence and angle of incidence) have no noticeable effect for the different beam profiles, here we focus on the different scanning directions i.e. scanning parallel and orthogonal to the polarization of the laser. The experiments for sapphire are carried out at normal incidence of the laser. Experiments show that qualitatively good one-dimensional LSFL are generated with a speed of 80 mm/s for the Gaussian beam profile and 120 mm/s for the Top-Hat beam profile, in both scanning directions. This different scanning speeds result in a pulse overlap of 95% for both beam profiles. Figure 6 compares SEM images of 1D-LSFL for (a) scanning orthogonal and (b) parallel to the polarization of the laser. The fluence is set to 4.6 J/cm² (E_p = 35.0 µJ) (orthogonal scanning) and 2.57 J/cm² (E_p = 19.4 µJ) (parallel scanning) for the Gaussian and 3.67 J/cm² (E_p = 74.3 µJ) (orthogonal scanning) and 3.33 J/cm² (E_p = 67.4 µJ) (parallel scanning) for the Top-Hat beam profile. Obviously, for both beam profiles, scanning orthogonal to the polarization of the laser requires a higher fluence. This behaviour is assigned, to a redistribution of the incident electric field of the laser by the initially induced structures, in turn causing an extension of the electric field distribution perpendicular to the LSFL [30] and is discussed in detail in Ref. 29 for the 1D-LSFL on sapphire. The different line width of the structures generated with the Gaussian beam is based on an interplay of the scanning direction and the laser beam polarization, while the orientation of the LSFL is found to be orthogonal to the polarization of the laser, independent of the scanning direction. Their periodicities in figure 6 reveal values of Λ_{LSFL} = 932 nm (Gaussian, orthogonal), Λ_{LSFL} = 965 nm (Gaussian, parallel), Λ_{LSFL} = 948 nm (Top-Hat, orthogonal) and Λ_{LSFL} = 987 nm (Top-Hat,

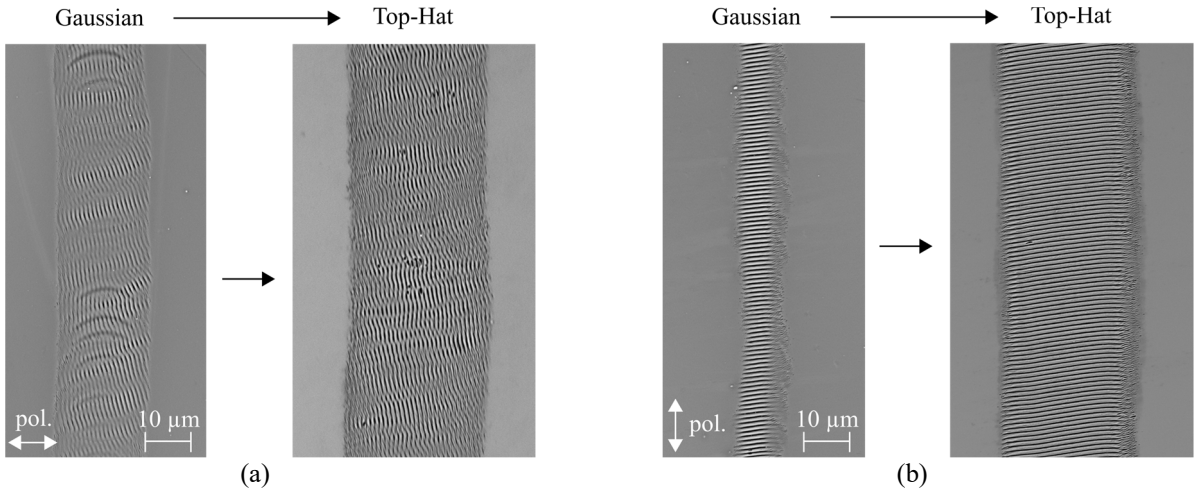

Fig. 6 SEM images of 1D-LSFL on sapphire, comparison of Gaussian (left) and Top-Hat (right) beam profiles for scanning (a) orthogonal and (b) parallel to the laser polarization.

parallel), thus being smaller than the laser wavelength. Comparing the one-dimensional structures generated orthogonal to the laser polarization reveal an improved quality, i.e. homogenous appearance of the LSFL. For the parallel scanning, a significantly increased line width is observed while the LSFL reveal excellent quality showing straight and homogeneous structures.

For both dielectric materials, we found an improved quality of the low spatial frequency LIPSS for the use of femtosecond beam-shaped laser profiles. A detailed evaluation of the fluence, pulse overlap and angle of incidence showed no influence of the different beam profiles. For fused silica an angular irradiation as well as the use of the Top-Hat increases the LSFL quality. Furthermore, the most homogenous LSFL can be generated on sapphire, scanning parallel to the polarization of the laser while using a Top-Hat beam-shaped laser profile.

4. Conclusion

We demonstrated the efficient fabrication of homogenous 1D-LSFL on dielectric materials, fused silica and sapphire. Comparing the fluence, the pulse overlap of the laser as well as the angle of incidence for the silica specimen, we found the same behaviour for the Gaussian and the Top-Hat profile. An angular irradiation is used for the homogeneous structuring of the fused silica samples, leading to an increased quality of the LSFL as well as an increased line width. For the sapphire, the scanning direction with regard to the laser polarization is investigated. For both, orthogonal and parallel scanning, an increased LSFL quality as well as line width for the Top-Hat profile is observed. The best quality is found for the parallel scanning case, also leading to the highest increase of line width compared to the Gaussian beams.

References

[1] M. Birnbaum: J. Appl. Phys., 36, (1965) 3688.
[2] J. E. Sipe, J. F. Young, J. S. Preston and H. M. van Driel: Phys. Rev. B, 27, (1983) 1141.
[3] A. Cunha, A. P. Serro, V. Oliveira, A. Almeida, R. Vilar and M.-C. Durrieu: Appl. Surf. Sci., 265, (2013) 688.
[4] J. Bonse, A. Rosenfeld and J. Krüger: J. Appl. Phys., 106, (2009) 104910.
[5] C. Albu, A. Dinescu, M. Filipescu, M. Ulmeanu and M. Zamfirescu: Appl. Surf. Sci., 278, (2013) 347.
[6] Z. Fang, Y. Zhao and J. Shao: Optik, 127, (2016) 1171.
[7] D. C. Emmony, R. P. Howson and L. J. Willis: Appl. Phys. Lett., 23, (1973) 598.
[8] Q. Sun, F. Liang, R. Vallée and S. L. Chin: Opt. Lett., 33, (2008) 2713.
[9] R. Kuladeep, C. Sahoo and D. N. Rao: App. Phys. Lett., 104, (2014) 222103.
[10] P. Bizi-Bandoki, S. Benayoun, S. Valette, B. Beaugiraud and E. Audouard: Appl. Surf. Sci., 257, (2011) 5213.
[11] F. Preusch, S. Rung and R. Hellmann: J. Laser Micro/Nanoeng., 11, (2016) 137.
[12] J. Eichstädt, G. R. B. E. Römer and A. J. Huis in't Veld: Phys. Procedia, 12, (2011) 7.
[13] S. Schwarz, S. Rung and R. Hellmann: Appl. Surf. Sci., 411, (2017) 113.
[14] R. Stoian, H. Varel, A. Rosenfeld, D. Ashkenasi, R. Kelly and E. E. B. Campbell: Appl. Surf. Sci., 165, (2000) 44.
[15] S. Rung, S. Schwarz, B. Götzendorfer, C. Esen and R. Hellmann: Appl. Sci., 8, (2018) 700.
[16] E. Rebollar, I. Frischauf, M. Olbrich, T. Peterbauer, S. Hering, J. Preiner, P. Hinterdorfer, C. Romanin and J. Heitz: Biomaterials, 29, (2008) 1796.
[17] K. Wallat, D. Dörr, R. Le Harzic, F. Stracke, D. Sauer, M. Neumeier, A. Kovtun, H. Zimmermann and M. Epple: J. Laser Appl., 24, (2012) 042016.
[18] X. Wang, C. A. Ohlin, Q. Lu and J. Hu: Biomaterials, 19, (2008) 2049.
[19] Z. Wang, Q. Zhao and C. Wang: Micromachines, 6, (2015) 1606.
[20] N. Yasumaru, K. Miyazaki and J. Kiuchi: Appl. Surf. Sci., 254 (2008) 2364.
[21] E. Granados, M. Martinez-Calderon, M. Gomez, A. Rodriguez and S. M. Olaizola: Opt. Express, 25, (2017) 15330.
[22] B. C. Stuart, M. D. Feit, A. M. Rubenchik, B. W. Shore and M. D. Perry: Phys. Rev. Lett., 74, (1995) 2248.
[23] S. K. Das, H. Messaoudi, A. Debroy, E. McGlynn and R. Grunwald, Opt. Mat. Express, 3, (2013) 1705.

[24] M. Huang, F. Zhao, Y. Cheng, N. Xu and Z. Xu, ACS Nano, 3, (2009) 4062.
[25] S. Gräf, C. Kunz and F. A. Müller: Materials, 10, (2017), 933.
[26] J. Bonse, J. Krüger, S. Höhm and A. Rosenfeld: J. Laser Appl., 24, (2012) 042006.
[27] D. Ashkenasi, A. Rosenfeld, H. Varel, M. Wähmer and E. E. B. Campbell: Appl. Surf. Sci., 120, (1997) 65.
[28] L. Qi, K. Nishii, M. Yasui, H. Aoki and Y. Namba: Opt. Lasers Eng., 48, (2010) 1000.
[29] S. Schwarz, S. Rung and R. Hellmann: J. Laser Micro/Nanoeng., 12, (2017) 67.
[30] C.-Y. Zhang, J.-W. Yao, C.-Q. Li, Q.-F. Dai, S. Lan, V. A. Trofimov and T. M. Lysak: Opt. Express, 21, (2013) 4439.

(Received: June 25, 2018, Accepted: September 6, 2018)